The North Pacific High and wintertime pre-conditioning of California current productivity

Isaac D. Schroeder,[1] Bryan A. Black,[2] William J. Sydeman,[3] Steven J. Bograd,[1] Elliott L. Hazen,[1] Jarrod A. Santora,[3] and Brian K. Wells[4]

Received 15 December 2012; accepted 17 December 2012.

[1] Variations in large-scale atmospheric forcing influence upwelling dynamics and ecosystem productivity in the California Current System (CCS). In this paper, we characterize interannual variability of the North Pacific High over 40 years and investigate how variation in its amplitude and position affect upwelling and biology. We develop a winter upwelling "pre-conditioning" index and demonstrate its utility to understanding biological processes. Variation in the winter NPH can be well described by its areal extent and maximum pressure, which in turn is predictive of winter upwelling. Our winter pre-conditioning index explained 64% of the variation in biological responses (fish and seabirds). Understanding characteristics of the NPH in winter is therefore critical to predicting biological responses in the CCS.
Citation: Schroeder, I. D., B. A. Black, W. J. Sydeman, S. J. Bograd, E. L. Hazen, J. A. Santora, and B. K. Wells (2013), The North Pacific High and wintertime pre-conditioning of California current productivity, *Geophys. Res. Lett.*, *40*, doi:10.1002/grl.50100.

1. Introduction

[2] Winter (January–March) coastal upwelling in the California Current System (CCS) has been associated with early phytoplankton production [*Chenillat et al.*, 2012], increased zooplankton abundance [*Dorman et al.*, 2011], and favorable physical and biological conditions for top predators including fish, seabirds, and mammals [*Logerwell et al.*, 2003; *Schroeder et al.*, 2009; *Black et al.*, 2010; *Thompson et al.*, 2012]. Winter upwelling is correlated with basin-scale atmospheric conditions represented by the Northern Oscillation Index [NOI; *Black et al.*, 2011], which in turn reflects variation in the North Pacific High (NPH) relative to other large-scale pressure systems in the Pacific Ocean [*Schwing et al.*, 2002]. The NPH is generally weak and centered farthest south in winter, but strengthens and migrates to more northerly latitudes at different rates and times each year [*Kenyon*, 1999]. This migration of the NPH is responsible for the annual strengthening of the equatorward winds that drive coastal upwelling in the summer. In this paper, we hypothesize that the positioning and amplitude of NPH determines winter upwelling and resulting biological processes in the central-northern CCS [*Sydeman et al.*, 2011]. Here, we quantify the mean and variance of NPH amplitude and positioning and relate these attributes to upwelling, proxied by the upwelling index, coastal sea level and coastal sea surface temperature (SST). We relate NPH metrics to fish and seabirds measurements to assess if measurements of NPH positioning, amplitude, and timing provide indices of "winter preconditioning" of the ecosystem. A final preconditioning index is developed that quantifies pulses of upwelling in the winter, which are sensitive to the amplitude and position of the NPH.

2. Data and Methods

[3] The U.S. Navy Fleet Numerical Meteorology and Oceanography Center (FNMOC) Sea Level Pressure (SLP) data were used to describe variation in the positioning and amplitude of the NPH (http://www.pfeg.noaa.gov/). Monthly averaged SLP values were obtained (1° × 1° resolution) for the period 1967 through 2010 ($n = 528$ months over 44 years). Time series of position and amplitude of the NPH were constructed from monthly SLP fields over the domain 160°W–110°W, 0°–50°N. We defined the position of the NPH as the center of the 1020 hPa isobar. To account for non-isotropic pressure distributions within the 1020 hPa isobar, the center of the SLP contained within the 1020 hPa contour was found by calculating the weighted mean:

$$\overline{x_k} = \frac{\sum_i^n p_{ik} x_{ik}}{\sum_i^n p_{ik}} \quad \overline{y_k} = \frac{\sum_i^n p_{ik} y_{ik}}{\sum_i^n p_{ik}}$$

where x_{ik} (y_{ik}) was the longitude (latitude) at time k and grid cell i, p_{ik} was the SLP at the location of (x_{ik},y_{ik}), and n was the total number of grid points within the 1020 hPa contour. If an SLP field for a given month did not have pressures above or equal to 1020 hPa, then the next lowest (decreasing by 0.5 hPa) level was used. Of the 528 months used, only 18 failed to have pressures above or equal to 1020 hPa. To quantify the amplitude of the NPH, two additional variables were calculated: (i) the areal extent of the 1020 hPa or equivalent isobar [$\boldsymbol{A}$ (km^2)] and (ii) the maximum SLP value contained within the 1020-hPa contour or equivalent isobar [$p_{\max}$ (hPa)].

[4] To identify how the positioning and amplitude of the NPH affects upwelling, the four variables outlined above ($\bar{x}$, $\bar{y}$, $\boldsymbol{A}$, and $p_{\max}$) were correlated with two upwelling response variables: coastal sea level and sea surface temperature. Data for the monthly time series of adjusted, detrended coastal sea level were obtained from the University of Hawaii Sea Level Center (http://uhslc.soest.hawaii.edu). Sea level anomalies at

[1]Environmental Research Division, SWFSC, NOAA, Pacific Grove, CA, USA.
[2]Marine Science Institute, University of Texas at Austin, Port Aransas, TX, USA.
[3]Farallon Institute for Advanced Ecosystem Research, Petaluma, CA, USA.
[4]Fisheries Ecology Division, SWFSC, NOAA, Santa Cruz, CA, USA.

Corresponding author: I. D. Schroeder, Environmental Research Division, SWFSC, NOAA, Pacific Grove, CA, USA. (isaac.schroeder@noaa.gov)

©2013. American Geophysical Union. All Rights Reserved.
0094-8276/13/10.1002/grl.50100

nine locations on the west coast were used: San Diego, CA; Port San Luis, CA; Monterey, CA; San Francisco, CA; Crescent City, CA; Charleston, OR; South Beach, OR; Astoria, OR and Neah Bay, WA. The lengths of the time series were different, but 6 out of 9 covered the 1967–2008 period. SST data were gridded (1° × 1° resolution) monthly averages compiled by the Met Office Hadley Centre's sea ice and SST data set (HadISST; http://coastwatch.pfeg.noaa.gov/erddap/index.html). We used the grid point located closest to the shore over the 32° to 48°N study region. To put the central–northern CCS region in broader context, we obtained daily upwelling indices [UI; *Bakun*, 1975; *Schwing et al*., 1996] for six locations (http://www.pfeg.noaa.gov) separated by three latitudes (33°N 119°W; 36°N 122°W; 39°N 125°W; 42°N 125°W; 45°N 125°W; and 48°N 125°W). These daily upwelling data were averaged with respect to month.

[5] To assess linkages with the broader Pacific basin, the area (***A***) of winter (January–February) NPH was compared to winter values of the Multivariate ENSO Index (MEI) as well as the North Pacific Index (NPI). The MEI [*Wolter and Timlin*, 2011] is an indicator of El Niño Southern Oscillation (ENSO) activity; positive values indicate El Niño conditions. The NPI is an indicator of the Aleutian Low, the dominant pressure system in the northeast Pacific during the winter, and is calculated by averaging the SLP over the 30°N–65°N, 160 E–140°W. Low NPI values indicate a more intense Aleutian Low [*Trenberth and Hurrell*, 1994].

[6] We calculated a direct index of winter "pre-conditioning," the pCUI, or pre-conditioning cumulative upwelling index, measured as the cumulative sum of only positive values of the daily UI between January 1 and March 1 each year. The pCUI was calculated for all UI locations mentioned above, but we focus on 39°N because most of the biological data used in this paper were collected near this latitude. We interpret the pCUI as an index of pulses in upwelling in January–February, which we relate to amplitude and positioning of the NPH. Time series of upper-trophic biological productivity were then compared to the pCUI.

[7] Next, we used Spearman's rank correlations (S_ρ) to associate the position and amplitude of the NPH (anomalies of the four NPH metrics after removing annual cycle) to the UI, pCUI and 4 biological time series that represent ecosystem productivity in the region. The biological time series were: the average annual egg-laying date for a planktivorous and omnivorous seabirds (Cassin's auklet and common murre), both datasets from Southeast Farallon Island (~37°N, ~123°W; data in *Schroeder et al*. [2009]), and otolith-based growth chronologies for planktivorous and piscivorous rockfishes (splitnose and yelloweye rockfish; data from *Black et al*. [2008, 2011]). On average auklets lay their eggs in April (standard of 15 days), and murres lay their eggs at the end of May (standard 9 days) [*Schroeder et al*., 2009]. The rockfish chronologies were derived from the widths of annual otolith increments; any value greater than one indicates above-average growth for that year [*Black et al*., 2008, 2011]. As top-level predators, seabirds and rockfish integrate bottom-up processes and show significant correlations with environmental variability and indices of lower-trophic variability [*Sydeman et al*., 2006; *Wells et al*., 2008; *Thompson et al*., 2012]. These four time series overlap spatially and temporally from 1973 to 2003. To reduce dimensionality of these time series, we normalized each and calculated their principal components, retaining those with an eigenvalue >1. The first PC ($PC1_{bio}$) explained 64% of the total variability and was the only PC to meet the criteria for inclusion in the subsequent analysis.

3. Results

[8] The NPH is of the lowest amplitude (low p_{max} and small ***A*** values), centered farthest south, and located the closest to land during January and February. It then intensifies, enlarges, and shifts northwestward through the spring and summer months (April–September) (Figure 1, Table 1). Variance in NPH location and strength is lowest during the summer and peaks from January through March (Figure 1). Area (***A***) shows the most within-month variability, especially in January and February with an interannual coefficient of variation of 95% and 85%, respectively. As expected, p_{max} shows little interannual variability within each month (Table 1). In

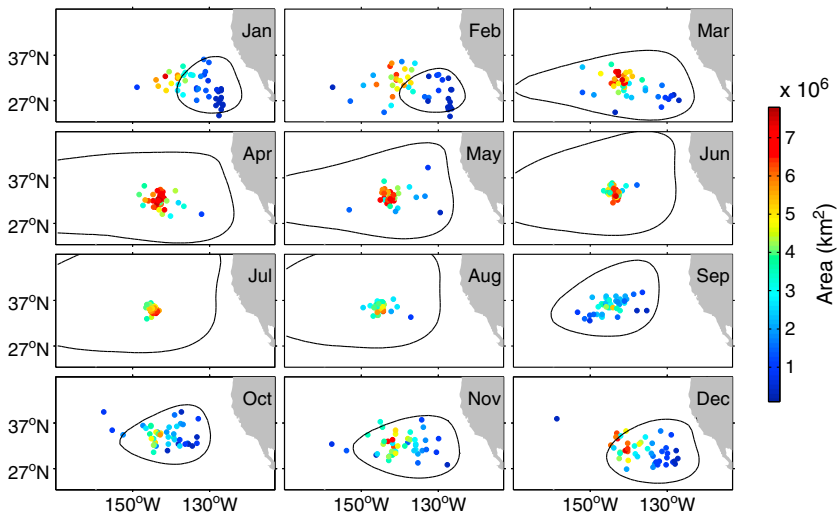

Figure 1. The position and amplitude of the North Pacific High (1967–2010) with respect to month. Each dot indicates the position of the NPH for a given year; color denoted the area of the 1020 hPa contour. The black contour is the climatological 1020 hPa isobar.

Table 1. Climatological means and coefficients of variation of the position ($\bar{x}$ and $\bar{y}$) and amplitude ($\boldsymbol{A}$ and p_{max}) of the NPH. The position of the NPH is defined as the weighted center of the 1020 hPa contour and the amplitude of the NPH is defined as the area of the 1020 hPa contour and the maximum value within the 1020 hPa

	Mean				Coefficient of Variation			
Month	$\bar{x}$ (°W)	$\bar{y}$ (°N)	$\boldsymbol{A}$ ($\times 10^6$ km^2)	p_{max} (hPa)	$\bar{x}$	$\bar{y}$	$\boldsymbol{A}$	p_{max}
January	133.6	30.2	2.15	1022.5	0.025	0.100	0.954	0.0031
February	136.7	30.1	2.51	1022.5	0.035	0.107	0.879	0.0031
March	140.1	30.5	3.91	1024.5	0.027	0.079	0.572	0.0032
April	142.8	32.2	5.51	1026.2	0.012	0.048	0.260	0.0023
May	141.8	33.0	4.92	1024.7	0.017	0.050	0.359	0.0022
June	143.7	34.0	5.12	1025.4	0.006	0.027	0.205	0.0019
July	144.8	35.1	5.03	1026.7	0.004	0.019	0.100	0.0020
August	144.9	35.5	4.26	1025.6	0.009	0.023	0.215	0.0024
September	144.7	35.9	2.50	1023.1	0.018	0.042	0.479	0.0021
October	141.6	34.4	2.48	1022.3	0.025	0.062	0.668	0.0016
November	139.9	32.3	3.15	1023.6	0.027	0.070	0.531	0.0022
December	136.5	31.1	2.78	1023.5	0.028	0.081	0.739	0.0027

terms of positioning, latitude ($\bar{y}$) shows more variability than longitude, especially during winter. Thus, the NPH center can be located as far south as 23°N or as far north as 36°N in winter; or it can be located in a coastal position (126°W) or farther offshore (157°W). The seasonal cycle of the four NPH variables $\bar{x}$, $\bar{y}$, $\boldsymbol{A}$, and p_{max} explain 38.0%, 51.3%, 34.5%, and 25.8% of the overall variance, respectively. When the seasonal signals are removed, all correlate with one another ($n = 528$, $p < 0.01$); longitude ($\bar{x}$) negatively relates to $\bar{y}$, $\boldsymbol{A}$, and p_{max} ($S_\rho = -0.22$, -0.32, and -0.44, respectively) such that the NPH center tends to be farther north, have higher maximum pressure, and a larger area when it is located farther from land (to the west). The highest correlation among variables is between $\boldsymbol{A}$ and p_{max} ($S_\rho = 0.81$), greater than those between $\bar{y}$ and the amplitude variables ($S_\rho = 0.31$ for $\boldsymbol{A}$ and 0.43 for p_{max}).

[9] Monthly averages of NPH position and amplitude significantly correlate with monthly averages of UI, sea level and SST over the course of the year. However, the strongest correlations among these variables occur between January and March (Figure 2). When the wintertime NPH is located to the northwest and has larger amplitude coastal upwelling is enhanced, and coastal sea level and SST decline. Time series of $\bar{y}$, $\boldsymbol{A}$, and p_{max} in January are significantly correlated with the time series of $\bar{y}$, $\boldsymbol{A}$, and p_{max} in February and March. Thus, NPH amplitude and latitudinal position show significant correlations from January into early spring. So, when the NPH is strong in January, it is likely to lead to enhanced upwelling in early spring.

[10] Our pre-conditioning index (pCUI) at 39°N ranges from 223 m^3 s^{-1} to 100 m^{-1} in 1983 to 4153 m^3 s^{-1} to 100 m^{-1} in 2007 (Figure 3a). The pCUI correlates ($p < 0.01$) to

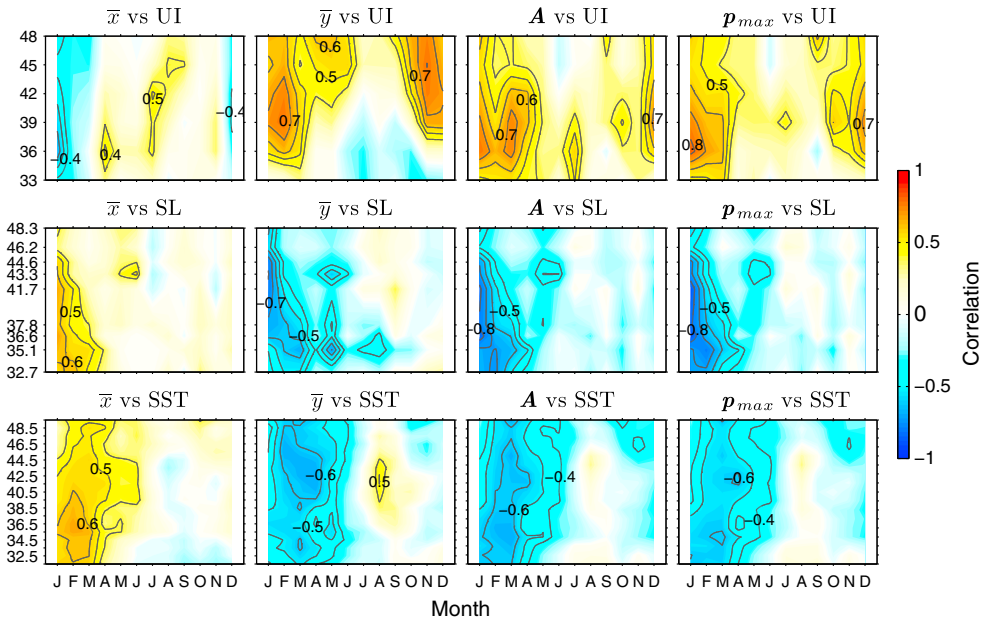

Figure 2. Spearman's rank correlations (S_ρ) between monthly time series of the NPH's position ($\bar{x}$ and $\bar{y}$) and amplitude ($\boldsymbol{A}$ and p_{max}) and: 1) top row: upwelling index at six different locations, 2) middle row: sea level from coastal tide gauges at eight different locations, and 3) bottom row: sea surface temperature means at 1° intervals along the coast. Black contours indicate significance at the $p < 0.01$ level.

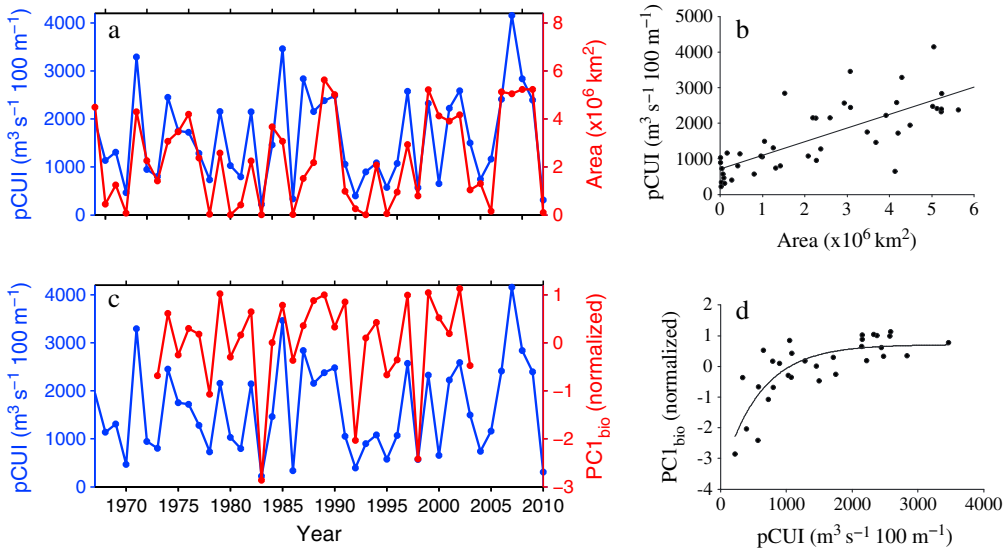

Figure 3. Time series and bivariate plots between the preconditioning cumulative upwelling index (pCUI) and: (a, b) January–February mean of the NPH's area and (c, d) $PC1_{bio}$, the leading principal component of four biological production indices that are sensitive to wintertime upwelling. The black line in the bivariate plots is a model fit.

January–February means of $\bar{x}$, $\bar{y}$, $\boldsymbol{A}$, and p_{max} with pairwise S_ρ correlations of −0.54, 0.65, 0.78, and 0.78, respectively. Of the four NPH variables, the January–February mean of $\boldsymbol{A}$ has the best fit with pCUI. Thus, area is the only variable retained when comparing NPH to atmospheric patterns and biological production. A linear model ($r^2 = 0.57$, $p < 0.01$) best describes the relationship between pCUI and the January–February mean of $\boldsymbol{A}$ (Figure 3b). Similar relationships between pCUI and the mean of January–February $\boldsymbol{A}$ occur at the other latitudes in the study region, but correlations are highest at 39°N. Area ($\boldsymbol{A}$) of the wintertime NPH also significantly negatively correlated with the winter MEI ($S_\rho = -0.64$; $p < 0.01$) and winter NPI ($S_\rho = 0.68$; $p < 0.01$). Thus, during the winter, the NPH area tends to be smaller during an El Niño and when the Aleutian Low is strong.

[11] The wintertime (January–February mean) NPH variables are significantly ($p < 0.05$) related to auklet lay-dates, splitnose rockfish growth and $PC1_{bio}$ (Table 2). Yelloweye growth is most poorly related to the NPH, with only one significant correlation ($\bar{y}$). The pCUI at 39°N is consistently related to all biological time series, especially $PC1_{bio}$ ($S_\rho = 0.76$; $p < 0.01$) (Table 2, Figure 3c). A non-linear model best fits the relationship between pCUI and $PC1_{bio}$, more specifically, an exponential to maximum diminishing returns model ($r^2 = 0.64$, $p < 0.01$; Figure 3d). A strong, northerly wintertime NPH is associated with early seabird lay dates, high fledgling survivorship, and vigorous rockfish otolith growth, all of which are consistent with elevated levels of productivity.

Table 2. Spearman's rank correlation between biological time series and the position ($\bar{x}$ and $\bar{y}$), the amplitude ($\boldsymbol{A}$ and p_{max}), and pCUI. Number of years in the biological time series is shown in parentheses; all fully overlap with physical time series. Correlations that are not significant at the $p < 0.05$ level are shaded

Biological Time Series	$\bar{x}$	$\bar{y}$	$\boldsymbol{A}$	p_{max}	pCUI
Auklet lay date (35)	0.50	-0.65	-0.74	-0.75	-0.74
Murre lay date (35)	0.21	-0.50	-0.40	-0.41	-0.54
Splitnose Growth (40)	-0.34	0.34	0.62	0.55	0.48
Yelloweye growth (37)	-0.08	0.44	0.27	0.30	0.49
PCI_{bio} (31)	-0.48	0.63	0.67	0.65	0.76

4. Discussion

[12] This paper builds upon a series of previous studies that document the importance of seasonality when considering physical-biological interactions in the California Current [e.g., *Bograd et al.*, 2009]. Indeed, upwelling in the central-northern CCS occurs in two distinct seasonal "modes" to which biological processes are differentially sensitive [*Black et al.*, 2011; *Thompson et al.*, 2012]. The long-term pattern of winter upwelling is punctuated by anomalies associated with ENSO, while summer upwelling is characterized by decadal oscillations and, at some latitudes, long-term increasing linear trends [*García-Reyes and Largier*, 2010; *Black et al.*, 2011]. As winter upwelling is generally weakest and primary productivity lowest, its relevance to biology has traditionally not been explored [but see *Logerwell et al.*, 2003]. Yet a growing number of recent studies document the importance of atmospheric-oceanographic coupling in winter (January–March) to ecosystem dynamics, including influences on both regional upwelling [*Black et al.*, 2011; *Thompson et al.*, 2012] and broad-scale effects on ocean currents [*Sydeman et al.*, 2011]. Unlike summer upwelling, winter upwelling strongly correlates to sea level pressure across a broad region of the North Pacific from the California coast to Hawaii [*Black et al.*, 2011], indicating that the North Pacific High may be the proximal atmospheric driver of wintertime upwelling and initial ecosystem productivity [*Bograd et al.*, 2002].

[13] *Bograd et al.* [2002] focused on describing trends, while here we have focused on quantifying interannual variability in the NPH. Interannual variability in the amplitude

and positioning of the winter NPH relates closely to interannual variability in winter upwelling, and is also reflected in coastal SST and sea level. Indeed, the sum of positive upwelling events in winter, which we develop as a preconditioning cumulative upwelling index or pCUI, is most closely related to the areal extent and maximum pressure of the NPH ($\boldsymbol{A}$, p_{max}). The pCUI also appears to be the most biologically-relevant measurement of this coherent winter climate pattern, as independently verified by multiple fish (rockfish) and seabird (auklet, murre) time series (Table 2). The underlying pCUI–biology relationship appears to be non-linear, and suggests an exponential response (Figure 3b). Extremely low values of pCUI exert a disproportionately strong influence on the biology of the system, while increasingly larger values result in diminishing returns in terms of the biological responses, which include growth, phenology (timing of breeding), and reproductive performance of the rockfish and seabird species. There is no apparent flattening of the response between $PC1_{bio}$ and the pCUI, indicating that this relationship is probably not asymptotic, but without more samples at the upper extent of the pCUI, this conclusion remains equivocal.

[14] The winter NPH is teleconnected to broad-scale atmospheric patterns in the tropical and extratropical Pacific Ocean as highlighted by its strong correlations to the MEI and NPI. Given the connection of this winter pattern across such broad regions and diverse physical indicators, the mechanisms that favor biological responses may be much more diverse than upwelling alone. High vales of the NPH could also be directly or indirectly associated with transport of water masses and associated plankton communities [*Keister et al*., 2011], latitude of the subarctic current bifurcation [*Sydeman et al*., 2011], or insolation and ocean stratification and associated properties of the water column. *Sydeman et al*. [2011] showed that when the NPH in April 2002 was greatly enlarged, the North Pacific Current shifted to the north with positive effects across multiple trophic levels of the CCS. Thus, the bio-physical interactions captured by the NPH are probably complex and integrate climate-ocean forcing over multiple spatial and temporal scales.

5. Conclusions

[15] Ultimately, we suggest that atmospheric conditions prior to what is formally known as the "spring transition" (the date at which the CCS shifts from southerly, downwelling-favorable winds to northerly, upwelling-favorable winds) are critical to ecosystem functions. The spring transition has been defined by various metrics including variation in sea level, sst, and upwelling [*Bograd et al*., 2009; *Holt and Mantua*, 2009], but fails to provide mechanistic understanding of ecosystem dynamics. Moreover, it is clear that the spring transition date is dependent on latitude, and in some regions where upwelling occurs year-round, defining a spring transition date is not possible. Here, we suggest that rather than emphasizing regionally variable dates per se, characterizing the period leading up to the general transition to upwelling-favorable conditions is more valuable for predicting winter-sensitive biological responses. Periods of upwelling-favorable conditions captured by measurements of the NPH and the pCUI provide a mechanism by which the atmosphere can affect the ocean at an important, yet often overlooked, time of year. Pulses in upwelling and nutrient influx in winter may elongate or provide an early start to the annual growing season [*Schroeder et al*., 2009], or a strong wintertime NPH may alter current flows which pre-condition the system in other ways [*Sydeman et al*., 2011]. In either case, decomposing the NPH in winter and developing the pCUI may serve as important early-season indicators for aspects of CCS productivity and underscore the importance of considering seasonality in key climatic and biological relationships in the CCS and perhaps other eastern boundary current systems worldwide.

[16] **Acknowledgments.** The seabird research was conducted and funded by PRBO Conservation Science on the Farallon National Wildlife Refuge, in collaboration with the US Fish and Wildlife Service. We thank PRBO and USFWS for data contributions to this project. Funding was provided by NOAA's Fisheries and the Environment (FATE) program, NOAA's California Current Integrated Ecosystem Assessment, and the National Science Foundation under grant 0929017. Special thanks to John Field and David Huff for reviewing earlier drafts of this manuscript.

References

Bakun, A. (1975), Daily and weekly upwelling indices, west coast of North America, 1967–1973, U.S. Dept. of Commerce, NOAA Tech. Rep., NMFS, Washington, DC.

Black, B. A., G. W. Boehlert, and M. M. Yoklavich (2008), Establishing climate-growth relationships for yelloweye rockfish (*Sebastes ruberrimus*) in the northeast Pacific using a dendrochronological approach, *Fish. Oceanogr.*, *17*(5), 368–379, doi:10.1111/j.1365-2419.2008.00484.x.

Black, B. A., I. D. Schroeder, W. J. Sydeman, S. J. Bograd, and P. W. Lawson (2010), Wintertime ocean conditions synchronize rockfish growth and seabird reproduction in the central California Current ecosystem, *Can. J. Fish. Aquat. Sci.*, *67*(7), 1149–1158, doi:10.1139/F10-055.

Black, B. A., I. D. Schroeder, W. J. Sydeman, S. J. Bograd, B. K. Wells, and F. B. Schwing (2011), Winter and summer upwelling modes and their biological importance in the California Current Ecosystem, *Glob. Change Biol.*, *17*, 2536–2545, doi:10.1111/j.1365-2486.2011.02422.x.

Bograd, S. J., F. B. Schwing, R. Mendelssohn, and P. Green-Jessen (2002), On the changing seasonality over the north Pacific, *Geophys. Res. Lett.*, *29*(9), doi:10.1029/2001GL013790.

Bograd, S. J., I. D. Schroeder, N. Sarkar, X. Qiu, W. J. Sydeman, and F. B. Schwing (2009), Phenology of coastal upwelling in the California Current, *Geophys. Res. Lett.*, *36*, 5, doi:10.1029/2008GL035933.

Chenillat, F., P. Rivière, X. Capet, E. D. Lorenzo, and B. Blanke (2012), North Pacific Gyre oscillation modulates seasonal timing and ecosystem functioning in the California Current upwelling system, *Geophys. Res. Lett.*, *39*, 6, doi:201210.1029/2011GL049966.

Dorman, J. G., T. M. Powell, W. J. Sydeman, and S. J. Bograd (2011), Advection and starvation cause krill (*Euphausia pacifica*) decreases in 2005 Northern California coastal populations: implications from a model study, *Geophys. Res. Lett.*, *38*, 5, doi:201110.1029/2010GL046245.

García-Reyes, M., and M. J. Largier (2010), Observations of increased wind-driven coastal upwelling off central California, *J. Geophys. Res.*, *115*, C04011, doi:10.1029/2009JC005576.

Holt, C. A., and N. Mantua (2009), Defining spring transition: regional indices for the California Current System, *Mar. Ecol. Prog. Ser.*, *393*, 285–299, doi:10.3354/meps08147.

Keister, J. E., E. Di Lorenzo, C. A. Morgan, V. Combes, and W. T. Peterson (2011), Zooplankton species composition is linked to ocean transport in the Northern California Current, *Glob. Change Biol.*, *17*, 2498–2511, doi:10.1111/j.1365-2486.2010.02383.x.

Kenyon, K. E. (1999), North Pacific High: an hypothesis, *Atmos. Res.*, *51*, 15–34.

Logerwell, E. A., N. Mantua, P. W. Lawson, R. C. Francis, and V. N. Agostin (2003), Tracking environmental processes in the coastal zone for understanding and predicting Oregon coho (*Oncorhynchus kisutch*) marine survival, *Fish. Oceanogr.*, *12*, 554–568, doi:10.1046/j.1365-2419.2003.00238.x.

Schroeder, I. D., W. J. Sydeman, N. Sarkar, S. A. Thompson, S. J. Bograd, and F. B. Schwing (2009), Winter pre-conditioning of seabird phenology in the California Current, *Mar. Eco.l Prog. Ser.*, *393*, 211–223, doi:10.3354/meps08103.

Schwing, F. B., T. Murphree, and P. M. Green (2002), The Northern Oscillation Index (NOI): a new climate index for the northeast Pacific, *Prog. Oceanogr.*, *53*(2–4), 115–139, doi:16/S0079-6611(02)00027-7.

Schwing, F. B., M. O'Farrell, J. Steger, and K. Baltz (1996), Coastal Upwelling Indices, West coast of North America, 1946–1995, U.S. Dept. of Commerce, NOAA Tech. Rep. Memo.

Sydeman, W. J., R. W. Bradley, P. Warzybok, C. L. Abraham, J. Jahncke, K. D. Hyrenbach, V. Kousky, J. M. Hipfner, and M. D. Ohman (2006), Planktivorous auklet *Ptychoramphus aleuticus* responses to ocean climate, 2005: Unusual atmospheric blocking?, *Geophys. Res. Lett.*, *33*, 5, doi:200610.1029/2006GL026736.

Sydeman, W. J., S. A. Thompson, J. C. Field, W. T. Peterson, R. W. Tanasichuk, H. J. Freeland, S. J. Bograd, and R. R. Rykaczewski (2011), Does positioning of the North Pacific Current affect downstream ecosystem productivity? *Geophys. Res. Lett.*, *38*, L12606, doi:10.1029/2011GL047212.

Thompson, S. A., W. J. Sydeman, J. A. Santora, B. A. Black, R. M. Suryan, J. Calambokidis, W. T. Peterson, and S. J. Bograd (2012), Linking predators to seasonality of upwelling: Using food web indicators and path analysis to infer trophic connections, *Prog. Oceanogr.*, *101*(1), 106–120, doi:10.1016/j.pocean.2012.02.001.

Trenberth, K. E., and J. W. Hurrell (1994), Decadal atmosphere-ocean variations in the Pacific, *Clim. Dynam.*, *9*, 303–319.

Wolter, K., and M. S. Timlin (2011), El Niño/Southern Oscillation behaviour since 1871 as diagnosed in an extended multivariate ENSO index (MEI.ext), *Int. J. Climatol.*, *31*, 1074–1087, doi:10.1002/joc.2336.

Wells, B. K., J. Field, J. Thayer, C. Grimes, S. Bograd, W. Sydeman, F. Schwing, and R. Hewitt (2008), Untangling the relationships among climate, prey, and top predators in an ocean ecosystem, *Mar. Ecol. Prog. Ser.*, *364*, 15–29, doi:10.3354/meps07486.